J Mater Sci (2007) 42:794–800
DOI 10.1007/s10853-006-0145-1

Mixed manganese spinel oxides: optical properties in the infrared range

N. Chasserio · B. Durand · S. Guillemet · A. Rousset

Received: 13 February 2006 / Accepted: 31 March 2006 / Published online: 12 January 2007

Abstract Spinel oxides in manganite family are studied in terms of optical properties in the infrared range (3–12 μm). The reflectivity is measured on sintered pellets. The complex refractive index is estimated by fitting hemispherical directional reflectance in both polarizations, perpendicular and parallel. The influence of different metallic cations (Ni, Co, Fe, Cu) is compared. In particular, in the case of manganese nickel copper oxides, the impact of variations in copper and nickel contents is evaluated. Cationic distribution is determined and correlated to the optical characteristics. These materials, usually used for NTC thermistor applications, are investigated for IR charges in coating.

Introduction

Optical properties of mixed oxides are studied within the framework of controlling the radiative properties of coatings. In particular, the aim of this work is to reduce the heating of device surfaces. This is conceivable if the materials in the coating present low absorbant capacities towards the surrounding radiations. For such applications, oxides have many interests in particular thanks to higher chemical and thermal stabilities than metallic charges presently used.

With the development of new soft chemistry routes, a wide variety of oxides can be prepared with a good control of the morphology and the grain size by changing transition metals or their respective content. This control is very important for the application in coatings, particularly for optical properties.

According to the relations between radiative properties and optical ones (Table 1), the oxides must exhibit complex refractive index with a high real part (relative to refraction) and a low imaginary part (relative to absorption) to be efficient. Some values are given in the literature for the visible range. For example, Shannon [1] indicated the real part of the refractive indexe of about 500 oxides at a wavelength of 589.3 nm. Only few data in the IR range (2–12 μm) are available in the literature. Some values, coming from Palik's handbooks [2] for simple or mixed oxides are reported in Table 2. However, no data concerning spinel oxides are available to our knowledge, except $MgAl_2O_4$. Moreover, none oxide exhibits high n and low k values.

We have first studied refractive indexes of various manganese spinel oxides. The synthesis of manganites and also ferrites has been thoroughly studied in our laboratory in order to better control composition, grain size and morphology of powders [3–6]. The present paper deals with the investigation of the optical properties of various manganese mixed oxides prepared by coprecipitation of oxalates and more especially with the influence of the chemical composition for the nickel copper manganese oxides which exhibit the best optical properties.

N. Chasserio (✉) · B. Durand · S. Guillemet · A. Rousset
Centre Interuniversitaire de Recherche et d'Ingénierie des Matériaux (CIRIMAT), CNRS UMR 5085, Laboratoire de Chimie des Matériaux Inorganiques et Energétiques, Université Paul Sabatier, 31062 Toulouse cedex 9, France
e-mail: chasserio@chimie.ups-tlse.fr

Table 1 Relations between optical and radiative properties

Optical properties	Radiative properties	Relations
Complex refractive index $N = n–i\ .\ k$		$\varepsilon = \frac{4 \cdot n}{(n+1)^2 + k^2}$ (null incidence)
Reflectivity R	Emissivity ε	$\varepsilon = \alpha = 1–R$
Absorptivity α		(Kirchhoff's laws, opaque ceramics)
Low emissivity↔Low absorptivity↔High reflectivity↔high n, low k (for oxides)		

Table 2 Example of oxide optical indexes (Palik's handbooks)

Oxides		λ (μm)	n	k	Oxides		λ (μm)	n	k
Al_2O_3	[7]	3.03	1.709	/	$MgAl_2O_4$	[8]	2.94	1.667	2.3×10^{-9}
	[9]	12.05	0.083	1.017			12.19	0.274	0.94
MgO	[10]	3.0	1.6915	1.1×10^{-7}	$LiNbO_3$	[11]	3.00	2.1625	/
	[12]	12.05	0.949	0.017×10^{-3}		[13]	12.50	0.20	1.24
BeO	[14, 15]	3.0	1.6798	/	$SrTiO_3$	[16]	3.03	2.221	/
	[17]	12.12	0.126	3.196			12.05	0.722	0.112
Cu_2O	[18]	3.0	2.55	/	$BaTiO_3$	[19]	3.03	2.25	2.97×10^{-2}
		12.0	2.37	/			12.05	1.23	2.84×10^{-2}

Experimental

Synthesis

Oxide powders were obtained by pyrolysis in air of mainly oxalate precursors, sometimes hydroxide ones (in the case of manganese copper oxide). These precursors were prepared at room temperature by the coprecipitation of aqueous solutions of transition metal salts using aqueous solution of ammonium oxalate (or sodium hydroxide) as precipitating agent. Starting metal salts were reagent grade chlorides except for the synthesis of hydroxide where nitrate reagents were used.

The precipitates were aged for 30 min under stirring, then filtered and washed several times with distilled water to eliminate chloride ions ($AgNO_3$ was added to the filtrate to control the presence of chlorides).

After decomposition, the oxide powders were mixed with a binder and dried at 80 °C. After grinding and sifting, powders were uniaxially pressed into pellets at a pressure of 100 MPa and sintered at the required temperature given in the references (Table 3). The optical characterizations were carried out on sintered materials so as to be representative of intrinsic properties of the materials.

Characterization

The chemical composition of the powders synthesized was controlled by Induced Coupled Plasma spectrometry (ICP). The relative error is 1%.

Table 3 Characteristics of bulk materials

Oxides	Densification (%)	Structure (Fig. 1)	Roughness (Ra μm)
$NiMn_2O_4$ [20]	93	Cubic	0.53
$CuMn_2O_4$ [21]	90	spine1	0.48
$Co_{0.27}Ni_{0.67}Mn_{2.06}O_4$ [22]	91		0.41
$Cu_{0.27}Ni_{0.68}Mn_{2.05}O_4$ [20]	95		0.45

The structure of the sintered pellets was characterized by X-Ray Diffraction with a Brüker D4 diffractometer using radiation Cu (K_α) (λ = 1.5418 Å).

The density was calculated from the mass and dimensions of the pellets.

Roughness was evaluated by interferential microscopy. Data were obtained by the MetroPro (Zygo Corporation) algorithm which gives the arithmetic roughness and cartography of the surface.

Optical characteristics were measured using a SOC-100 measurement system that consists of three separated but integrated components. The reflectance and transmittance measurements were performed with a SOC-100 hemispherical directional reflectometer. The Nicolet Magna 550 spectrophotometer FTIR provided the spectral data acquisition functions which mate directly to the SOC-100 HDR. The computer provides for the control of both FTIR and SOC-100 HDR. In the following, the hemispherical directional reflectance is noted HDR. The relative uncertainty on HDR, measured on many sintered pellets, is 5%.

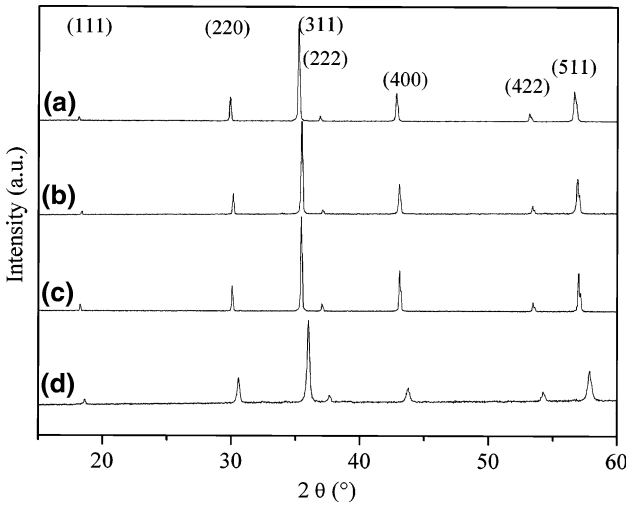

Fig. 1 XRD patterns of manganites (**a**) Mn–Ni (**b**) Mn–Ni–Co (**c**) Mn–Ni–Cu (**d**) Mn–Cu

The constants, n and k, were determined by fitting the HDR data to calculated ones which are functions of n and k, polarization and incident angle. Several measurements carried out for both polarizations (s and p) were then used to calculate bulk optical constants. The software Film Wizard was used to perform this fitting. The root mean squared error (RMSE), which gives the difference between measurement and fit, is in all cases, less than 0.5.

The emissivity was measured to check the good agreement between optical and radiative characteristics as mentioned in Table 1. This was made using a test bed in which an IR detector measures the ratio of brightness between the sample and a black body (a part of the sample covered by an absorbant coating), together at the same temperature. The detector is made of two materials: HgCdTe and InSb, active at different wavelengths in IR range (peaks of detection: 5 μm for InSb, 12 μm for HgCdTe).

Results

Manganese spinel oxides

In this section, the optical properties determined for some manganites, $M_xMn_{3-x}O_4$ (with M = Ni, Cu, Ni + Co or Ni + Cu), are given. Manganese content is equivalent in all cases. Bulk properties of characterized ceramics are reported in Table 3.

As optical properties are dependant of surface quality, we have checked that roughness is equivalent for all pellets. The differences between obtained values, reported in Table 3, are not significant enough to induce significant changes in optical measurements [23].

The X-ray diffraction patterns of the different ceramics (Fig. 1) only show a cubic spinel phase. For all the synthesized powders, the micrographies reveal octahedral particles as shown in Fig. 2 in the case of manganese nickel copper oxide.

The Fig. 3 represents the hemispherical directional reflectance of the sintered previous oxides, for an incident angle $\theta = 10°$, measured at different wavelengths. The corresponding optical indexes are reported in Table 4.

The reflectivity R calculated from the experimental emissivity (see Table 1: $R = 1–\varepsilon$) was in good agreement with the measured reflectivity, and the emissivity will therefore not be discussed any further.

As observed in Fig. 3, the nature of the cations in the structure highly affects the HDR measurements.

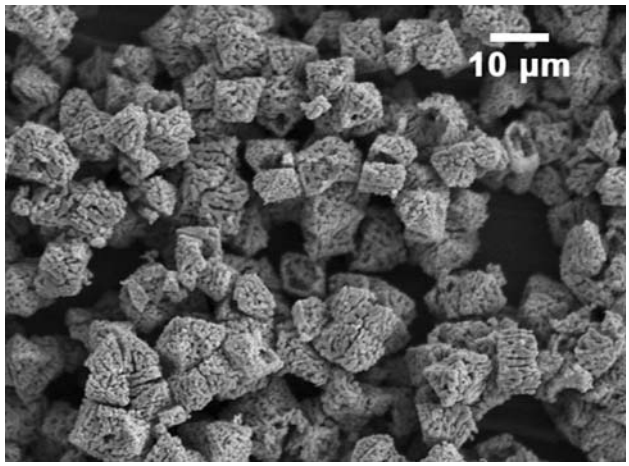

Fig. 2 Scanning Electron Micrograph of manganese nickel copper oxide decomposed at 900 °C

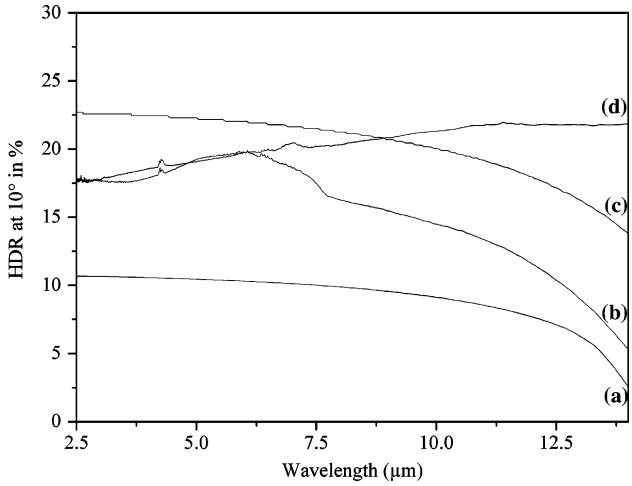

Fig. 3 Hemispherical Directional Reflectance HDR(10°) of manganites as a function of wavelength (**a**) Mn–Ni (**b**) Mn–Ni–Co (**c**) Mn–Ni–Cu (**d**) Mn–Cu

Table 4 Optical indexes of manganites

Wavelength	3 μm		5 μm		8 μm		12 μm	
Systems	n	k	n	k	n	k	n	k
(a) Mn–Ni	1.97	10^{-3}	1.96	10^{-3}	1.92	2.8×10^{-3}	1.77	2.4×10^{-3}
(b) Mn–Ni–Co	2.46	10^{-3}	2.58	5.4×10^{-3}	2.46	2.5×10^{-3}	2.12	3.8×10^{-3}
(c) Mn–Ni–Cu	2.85	10^{-3}	2.84	9×10^{-3}	2.79	1.9×10^{-3}	2.47	10^{-2}
(d) Mn–Cu	2.48	10^{-3}	2.62	10^{-3}	2.70	1.5×10^{-3}	2.78	2×10^{-3}

Considering the introduction by substitution of cobalt in nickel manganite, it is observed that the reflectivity is increased from 11% to about 17% at $\lambda = 2.5$ μm. The curve presents a peak of reflectivity at $\lambda \approx 5.5$ μm.

The substitution by copper increases the HDR to 22%. This cation seems to have a particular effect. In fact, a copper manganese oxide has a different behaviour in that HDR increases with the wavelength.

In terms of optical indexes, a high value of refractive index n is obtained for manganese nickel copper oxide, up to 2.85 at $\lambda = 3$ μm.

Manganese nickel copper oxides

In this section, we focus on the Mn–Ni–Cu spinel oxides that present the highest n value with an intermediate k value. This system shows the best compromise for our application. The influence of the different contents of metal cations in this system is studied.

Four compositions have firstly been tested (as reported in Table 5) in order to quantify the copper content effects in Mn–Ni–Cu oxides. So, nickel content has been held approximately constant.

The optical measurements (Fig. 4) show that the reflectivity first increases then decreases with the increase of copper content. The highest values for all wavelengths were obtained for a molar content close to 0.35.

In order to estimate the influence of nickel content on reflectivity, a second series of compositions has been tested (Table 6). The highest copper content was choosen in order to evaluate if the variation of nickel content can allow to thwart the decrease.

As for the influence of copper content, the curve (Fig. 5) successively presents an increase and a decrease on both sides of nickel content about 0.50. The optimal composition is for nickel content 0.52. The HDR is then about 30% for $\lambda = 3$ μm.

Table 5 Copper contents in Mn–Ni–Cu oxides for Ni = 0.7

Cu	0.10	0.27	0.35	0.44
Ni		0.70 ± 0.04		
Mn	2.24	2.05	1.92	1.87

The increase of copper content to 0.44 (Fig. 4) associated with a decrease of nickel content from 0.7 to about 0.5 leads to increased optical properties. The

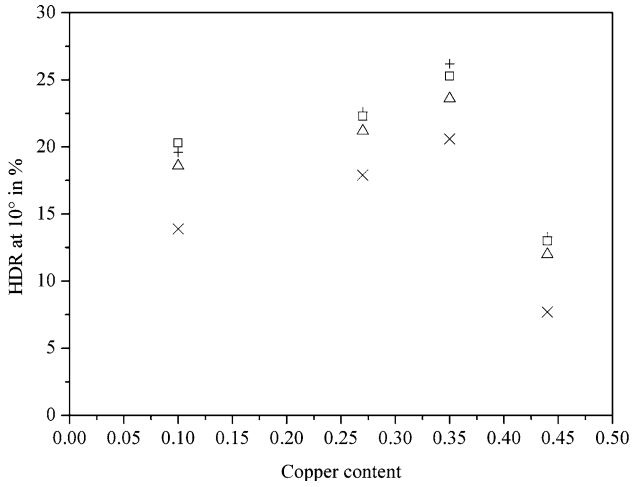

Fig. 4 Influence of Cu content on HDR (Ni = 0.7) at $\lambda = 3$ (□), 5 (+), 8 (△) and 12 (×) μm

Table 6 Nickel contents in Mn-Ni-Cu oxides for Cu = 0.44

Ni	0.69	0.52	0.43
Cu		0.44 ± 0.04	
Mn	1.87	2.03	2.13

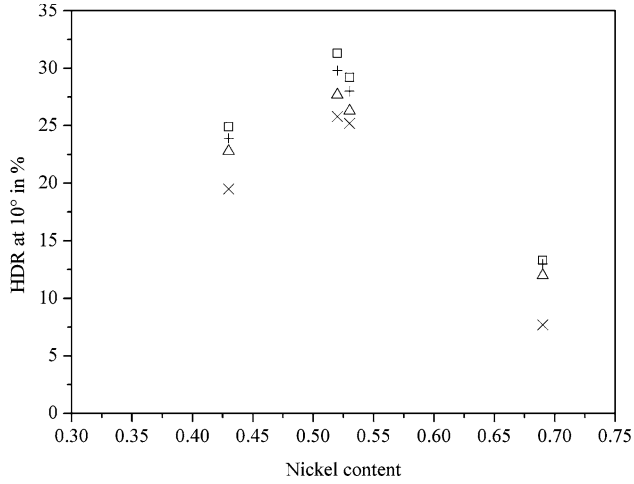

Fig. 5 Influence of Ni content on HDR (Cu = 0.44) at $\lambda = 3$ (□), 5 (+), 8 (△) and 12 (×) μm

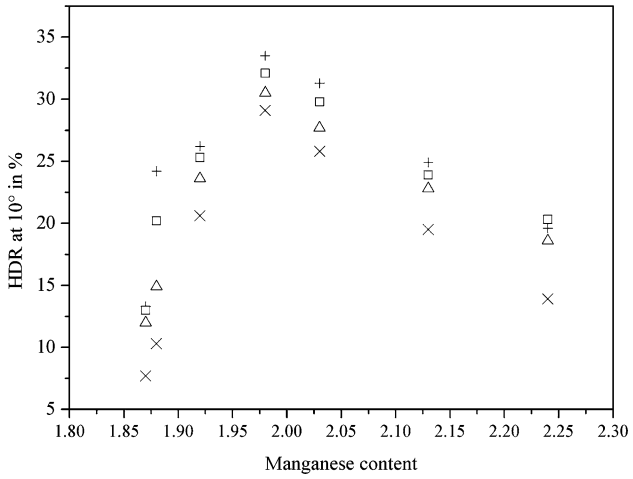

Fig. 6 Influence of Mn content on HDR at λ = 3 (□), 5 (+), 8 (△) and 12 (×) μm

influence of manganese is reported in Fig. 6. The evolution of the HDR values is similar to the previous ones. The highest HDR is obtained for a mixed oxide that contains a molar content of manganese close to 2.

Considering the successive influences of the metallic cations nickel, copper and manganese, it appears that the composition strongly influences the reflective properties of the oxide.

Discussions

In spinel oxides, many authors have shown that a variation in the distribution of cations in tetrahedral and octahedral sites involves significant changes in some of the physical properties (electric [24, 25], magnetic [6, 26]...). The cationic distribution in nickel copper manganites has often been studied [24, 27–29]. It is well established that nickel cation is only bivalent. XPS measurements [24, 29] showed that copper can exist in both sites as monovalent and bivalent. Manganese can be bi-, tri- and tetra-valent [29]. In the example of the Ni-substitution in hausmanite $Mn_3O_4\left(Mn^{2+}\left[Mn_2^{3+}\right]O_4^{2-}\right)$, the substitution can occur in tetrahedral or octahedral positions. The conservation of electroneutrality in octahedral sites implies the formation of Mn^{4+} cations. It is worthwhile noting that tetravalent manganese cations have a marked preference for octahedral sites. The localization of the other cations is still discussed. Navrotsky and Kleppa [30] calculated, from thermodynamic measurements, the site preference energy of several cations within the spinel structure. If Cu^{2+}, Ni^{2+} and Mn^{3+} prefer octahedral environment, Mn^{2+} prefers tetrahedral one. But, some authors [31] concluded, from neutron diffraction experiments, that Ni^{2+} can also exist in tetrahedral position. Drouet et al. [29] have shown that Cu^{2+} can occupy both sites.

For copper nickel manganites $Cu_xNi_{0.7}Mn_{2.3-x}O_4$, Caffin [32] and Guillemet-Fritsch [24, 33] have proposed the cationic distributions reported in Table 7. As the copper content increases up to 0.32, two parallel changes occur in the cationic distribution: $Cu_{Oh}^{2+} \rightarrow Cu_{Td}^{2+}$ and $Ni_{Td}^{2+} \rightarrow Ni_{Oh}^{2+}$. At the same time, the optical property HDR increases (Fig. 4). For higher copper content, the nickel cations only occupy octahedral sites and copper could be present in two valences.

For the composition $x = 0.10$, a different cooling rate after the sintering process has been performed (6 °C/h against 80 °C/h before). HDR data are reported in Fig. 7. For slow cooling rate, Boucher et al. [35] have shown that $Ni_{Td}^{2+} \rightarrow Ni_{Oh}^{2+}$, site where nickel is more stable according to Navrotsky and Kleppa. But the HDR decreases as the cooling rate decreases. So in the hypotheses we made $\left(Cu_{Oh}^{2+} \rightarrow Cu_{Td}^{2+} \text{ and } Ni_{Td}^{2+} \rightarrow Ni_{Oh}^{2+}\right)$,

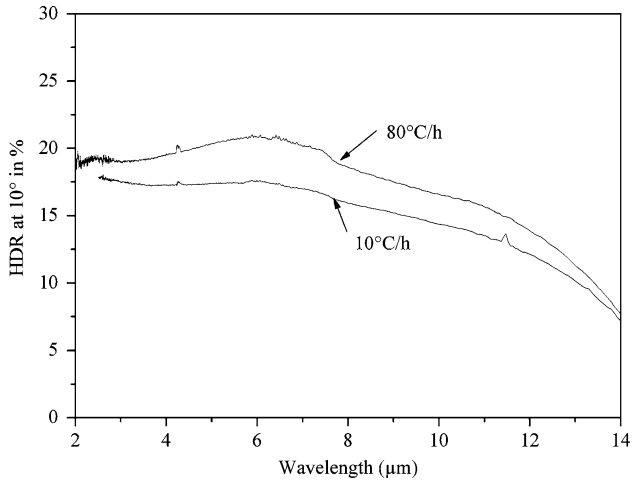

Fig. 7 Cooling rate influence on HDR (Cu = 0.10)

Table 7 Cationic distributions in nickel copper manganites

Cu content	Ni content	Mn content	Cationic distribution	Ref
0.13	0.70	2.17	$Cu_{0.07}^{2+}\ Ni_{0.06}^{2+}Mn_{0.87}^{2+}\ [Cu_{0.06}^{2+}Ni_{0.64}^{2+}Mn_{0.6}^{3+}Mn_{0.7}^{4+}]O_4^{2-}$	[32, 33]
0.23	0.70	2.07	$Cu_{0.16}^{2+}Ni_{0.07}^{2+}Mn_{0.77}^{2+}[Cu_{0.07}^{2+}Ni_{0.63}^{2+}Mn_{0.6}^{3+}Mn_{0.3}^{4+}]O_4^{2-}$	
0.32	0.70	1.98	$Cu_{0.32}^{2+}Mn_{0.60}^{2+}[Ni_{0.3}^{2+}Mn_{0.6}^{3+}Mn_{0.31}^{4+}]O_4^{2-}$	
0.41	0.66	1.93	$Cu_{0.36}^{2+}Mn_{0.616}^{2+}Cu_{0.024}^{+}[Cu_{0.026}^{2+}Ni_{0.660}^{2+}Mn_{0.604}^{3+}Mn_{0.310}^{4+}]O_4^{2-}$	[34]

Table 8 Cationic distributions in nickel copper manganites

Cu content	Ni content	Mn content	Cationic distribution	a (Å)	Ref
0.5	0.5	2.0	$Cu^{+}_{0.22}Mn^{2+}_{0.68}Mn^{3+}_{0.1}[Cu^{2+}_{0.28}Ni^{2+}_{0.5}Mn^{3+}_{0.32}Mn^{4+}_{0.9}]O^{2-}_{4}$	8.373	[27]
0.5	0.4	2.0	$Cu_{0.35} + Mn^{3+}_{0.65}[Cu^{2+}_{0.25}Ni^{2+}_{0.4}Mn^{3+}_{1.00}Mn^{4+}_{0.35}]O^{2-}_{4}$	8.34	[28]

we may assume that the main influence is given by the presence of copper cations.

In the second part, we have studied the influence of nickel content (Fig. 5). The maximum HDR measured here was for copper content = 0.44 and nickel content = 0.52. The calculated lattice parameter is 8.368 Å.

Trollund et al. [27] and Bhandage et al. [28] have proposed the cationic distributions reported in Table 8.

Regarding the lattice parameter we have measured and the ones given in Table 8 and the difference between the two compositions, we suggest in our case that Cu^{+} and Cu^{2+} coexist but in two different sites for the composition Cu = 0.44 and Ni = 0.52 as given by Trollund [27] in Table 8. Optical properties are enhanced.

Conclusions

This study has allowed to establish data of refractive indexes, in the infrared range, for mixed oxides with spinel structure, that are missing in the literature. Moreover, refractive indexes with high real part have been obtained for manganite spinel thanks to the presence of copper. In fact, in mixed spinel oxides systems with manganese, nickel and copper, refractive indexes close to 2.8 (for $\lambda = 3$ μm) have been reached.

The various compositions of nickel copper manganites lead to various optical properties. This point is of interest because the control of composition permits to adjust HDR.

Future study of the cationic distribution might allow to find a microscopic explanation. In fact, optical properties depend on the composition through the cation valencies and the sites they occupy.

The optimisation of optical properties seems to be obtained for copper in both valencies and both sites. New compositions must be tested to find the optimized ratio Cu^{+}_{Td}/Cu^{2+}_{Oh} and to evaluate the influence of the nickel cations.

Acknowledgements The authors are grateful to DGA for financially support this work. They also thank B. Berton, N. Vukadinovic and Olivier Calvo-Perez (Dassault Aviation, France) and L. Sauques, P. Sigaud and T. Dubois (Centre Technique d'Arcueil, France) for their help in optical measurements.

References

1. Shannon RD, Shannon RC, Medenbach O, Fischer RX (2002) Journal of physical and chemical reference data 31:931
2. Palik ED Handbook of optical constants of solids (I,II)
3. Battault T, Legros R, Rousset A (1995) Journal of european ceramic society 15:1141
4. Chanel C, Fritsch S, Drouet C, Rousset A, Sarrion MLM, Mestres L, Morales M (2000) Materials research bulletin 35:431
5. Drouard S, Tailhades P, Rousset A (1997) Comptes rendus de l'académie des sciences-Série IIB-Mechanics-Physics-Chemistry-Astronomy 325:739
6. Villette C, Tailhades P, Rousset A (1995) Journal of solid state chemistry 117:64
7. Maliston IH, Murphy FV, Rodeny WS (1958) Journal of optical society of America 48:72
8. Thomas ME (1989) SPIE 1112
9. Barker AS (1963) Physical review 132:1474
10. Herzberger MH, Salzberg CD (1962) Journal of optical society of America 52:240
11. Boyd GD, Miller RC, Nassau K, Bond WL, Savage A (1964) Applied physics letters 5:934
12. Piriou B, Cabannes F (1968) Optical acta 15:271
13. Axe JD, O'Kane DF (1966) Applied Physics Letters 9:58
14. Herzberger M (1958) Optical acta 6:197
15. Herzberger M, Salzberg CD (1962) Journal of optical society of America 52:420
16. Servoin JL, Luspin Y, Gervais F (1980) Physical review B 22:5501
17. Loh E (1968) Physical review 166:673
18. O'Keeffe MI (1963) Journal of Chemical Physics 39:1789
19. Servoin JL, Gervais F, Quittet AM, Luspin Y (1980) Physical review B 21:2038
20. Caffin JP, Rousset A, Carnet R, Lagrange A (1987) Materials science monograph 380:1743
21. Jarrige J, Mexmain J (1976) Bulletin de la société chimique de France 3–4:405
22. Battault T (1996) Journal of material synthesis and processing 4:361
23. Hervé P, Techniques de l'ingénieur, Vol. Mesures Physiques/ Grandeurs thermiques R 2 7371
24. Elbadraoui E, Baudour JL, Bouree F, Gillot B, Fritsch S, Rousset A (1997) Solid state ionics 93:219
25. Battault T, Legros R, Rousset A (1995) Journal of the european ceramic society 15:1141
26. Rousset A (1996) Solid state ionics 84:293
27. Trollund E, Chartier P, Gautier J-L (1990) Electrochimica acta 35:1303
28. Bhandage GT, Keert HV (1976) Journal of physics C 9:1325

29. Drouet C, Laberty C, Fierro JLG, Alphonse P, Rousset A (2000) International journal of inorganic materials 2:419
30. Navrotsky A, Kleppa OJ (1967) Journal of inorganic nuclear chemistry 29:2701
31. Meenakshisundaram A, Gunasekaram N, Srinvasan V (1982) Physica status solidi a 68
32. Caffin J-P (1986) thesis, Université Paul Sabatier (Toulouse)
33. Fritsch S (1995) thesis, Université Paul Sabatier (Toulouse)
34. Elbadraoui E, Baudour JL, Bouree F, Gillot B, Fritsch S, Rousset A (1997) Solid state ionics 93:219
35. Boucher R, Buhl R, Perrin M (1969) Acta cristallographica B 25:2326